



Universiteit  
Leiden  
The Netherlands

## **Short-term preoperative protein restriction attenuates vein graft disease via induction of cystathionine gamma-lyase**

Trocha, K.M.; Kip, P.; Tao, M.; MacArthur, M.R.; Trevino-Villarreal, J.H.; Longchamp, A.; ... ; Ozaki, C.K.

### **Citation**

Trocha, K. M., Kip, P., Tao, M., MacArthur, M. R., Trevino-Villarreal, J. H., Longchamp, A., ... Ozaki, C. K. (2020). Short-term preoperative protein restriction attenuates vein graft disease via induction of cystathionine gamma-lyase. *Cardiovascular Research*, 116(2), 416-428. doi:10.1093/cvr/cvz086

Version: Publisher's Version

License: [Creative Commons CC BY 4.0 license](#)

Downloaded from: <https://hdl.handle.net/1887/3181288>

**Note:** To cite this publication please use the final published version (if applicable).

# Short-term preoperative protein restriction attenuates vein graft disease via induction of cystathionine $\gamma$ -lyase

Kaspar M. Trocha<sup>1,2†</sup>, Peter Kip<sup>1,2,3†</sup>, Ming Tao<sup>1</sup>, Michael R. MacArthur<sup>2</sup>, J. Humberto Treviño-Villarreal<sup>2</sup>, Alban Longchamp<sup>1,2</sup>, Wendy Toussaint<sup>4,5</sup>, Bart N. Lambrecht<sup>4,5</sup>, Margreet R. de Vries<sup>3</sup>, Paul H.A. Quax<sup>3</sup>, James R. Mitchell<sup>2\*</sup>, and C. Keith Ozaki<sup>1\*</sup>

<sup>1</sup>Department of Surgery and the Heart and Vascular Center, Brigham & Women's Hospital and Harvard Medical School, 75 Francis Street, Boston, MA 02115, USA; <sup>2</sup>Department of Genetics and Complex Diseases, Harvard T.H. Chan School of Public Health, Boston, MA 02115, USA; <sup>3</sup>Eindhoven Laboratory for Experimental Vascular Medicine and Department of Surgery, Leiden University Medical Center, Leiden, the Netherlands; <sup>4</sup>VIB-UGent Center for Inflammation Research, and Department of Internal Medicine and Pediatrics, Ghent University, Belgium and <sup>5</sup>Department of Internal Medicine, Ghent University, Ghent, Belgium

Received 12 August 2018; revised 4 March 2019; editorial decision 23 March 2019; accepted 27 March 2019; online publish-ahead-of-print 29 March 2019

Time for primary review: 69 days

## Aims

Therapies to prevent vein graft disease, a major problem in cardiovascular and lower extremity bypass surgeries, are currently lacking. Short-term preoperative protein restriction holds promise as an effective preconditioning method against surgical stress in rodent models, but whether it can improve vein graft patency after bypass surgery is undetermined. Here, we hypothesized that short-term protein restriction would limit vein graft disease via up-regulation of cystathionine  $\gamma$ -lyase and increased endogenous production of the cytoprotective gaseous signalling molecule hydrogen sulfide.

## Methods and results

Low-density lipoprotein receptor knockout mice were preconditioned for 1 week on a high-fat high-cholesterol (HFHC) diet with or without protein prior to left common carotid interposition vein graft surgery with caval veins from donor mice on corresponding diets. Both groups were returned to a complete HFHC diet post-operatively, and vein grafts analysed 4 or 28 days later. A novel global transgenic cystathionine  $\gamma$ -lyase overexpressing mouse model was also employed to study effects of genetic overexpression on graft patency. Protein restriction decreased vein graft intimal/media+adventitia area and thickness ratios and intimal smooth muscle cell infiltration 28 days post-operatively, and neutrophil transmigration 4 days post-operatively. Protein restriction increased cystathionine  $\gamma$ -lyase protein expression in aortic and caval vein endothelial cells (ECs) and frequency of lung EC producing hydrogen sulfide. The cystathionine  $\gamma$ -lyase inhibitor propargylglycine abrogated protein restriction-mediated protection from graft failure and the increase in hydrogen sulfide-producing ECs, while cystathionine  $\gamma$ -lyase transgenic mice displayed increased hydrogen sulfide production capacity and were protected from vein graft disease independent of diet.

## Conclusion

One week of protein restriction attenuates vein graft disease via increased cystathionine  $\gamma$ -lyase expression and hydrogen sulfide production, and decreased early inflammation. Dietary or pharmacological interventions to increase cystathionine  $\gamma$ -lyase or hydrogen sulfide may thus serve as new and practical strategies to improve vein graft durability.

## Keywords

Vascular disease • Cardiovascular surgery • Diet and nutrition

\* Corresponding author. Tel: +1 857 307 1920; fax: +1 857 307 1922, E-mail: CKOzaki@partners.org (C.K.O.); Tel: +1 617 4327286; E-mail: jmitchel@hsph.harvard.edu (J.R.M.)

<sup>†</sup> The first two authors are co-first authorship.

Published on behalf of the European Society of Cardiology. All rights reserved. © The Author(s) 2019. For permissions, please email: journals.permissions@oup.com.

# 1. Introduction

Lifestyle choices such as diet contribute to the development and progression of atherosclerosis and cardiovascular disease<sup>1,2</sup> requiring lower-extremity or coronary bypass surgery.<sup>3,4</sup> Harvesting a suitable venous conduit and transplanting it into an arterial circuit induces a cascade of biologic events including ischaemia–reperfusion injury, oxidative stress, and acute biomechanical perturbations such as increased wall shear stress.<sup>5,6</sup> The subsequent adaptation to an arterial environment continues to stimulate endothelial cells (ECs) following transplantation,<sup>7</sup> in turn up-regulating various pro-inflammatory surface markers such as vascular cell adhesion molecule (VCAM) and intercellular adhesion molecule (ICAM).<sup>8,9</sup> Circulating leucocytes then attach to adhesion molecules and transmigrate across the luminal wall,<sup>8,10</sup> initiating a cascade leading to intimal hyperplasia (IH) and vein graft occlusion.<sup>11</sup> Although autogenous vein grafts remain superior to prosthetic conduits for lower-extremity bypass grafting,<sup>12,13</sup> nearly 40% of autogenous vein grafts will develop IH and subsequently occlude over time, leading to reinterventions, amputation, myocardial infarction, or death.<sup>13</sup> While the prospect of engineered decellularized vascular grafts appears promising as a conduit option,<sup>14</sup> currently, the most durable vascular graft for peripheral arterial bypass remains the autogenous vein graft.<sup>13,15</sup> Furthermore, patients with multivessel coronary artery disease are best treated with coronary artery bypass grafting (CABG), in which >90% necessitate both arterial and vein grafts as bypass conduits to revascularize ischaemic myocardium.<sup>16,17</sup> Yet, no significant therapies have been developed to prevent vein graft disease.

Defining mechanisms of IH and employing novel strategies to attenuate the fibroproliferative response are thus critical in order to improve revascularization surgery outcomes. Emerging basic science and clinical trials point to the promise of brief pre-operative dietary restriction as an intervention with the potential to improve surgical outcomes,<sup>18,19</sup> even in elective cardiovascular surgery patients who have high rates of post-operative morbidity and mortality.<sup>20</sup> Such dietary interventions are rooted in the field of aging and lifespan extension by nutrient/energy restriction,<sup>21–23</sup> which was first shown to reduce the incidence of cancer in rodents over a century ago,<sup>24</sup> and include reducing total calorie intake, intermittent fasting, or dilution of dietary components such as protein or amino acids.<sup>25</sup>

Recently, we reported numerous benefits of dietary restriction preconditioning in pre-clinical rodent surgical models of ischaemia–reperfusion injury to various organs, revascularization following femoral ligation, and IH following focal stenosis<sup>26–31</sup> without decelerating the post-intervention wound healing process.<sup>32</sup> On a mechanistic level, short-term dietary restriction interventions induce pleotropic and rapid changes in metabolism<sup>27,33,34</sup> and immune function<sup>35</sup> that in the surgical context can be anti-inflammatory and promote stress resistance.<sup>23</sup> For example, dietary preconditioning against hepatic ischaemia–reperfusion injury or femoral ligation in mice involves up-regulation of cystathionine  $\gamma$ -lyase (CGL), also known as CTH or CSE and endogenous production of hydrogen sulfide ( $H_2S$ ),<sup>26</sup> a dynamic mediator of vascular homeostasis.<sup>36,37</sup> At least two other enzymes, cystathionine  $\beta$ -synthase (CBS) and 3-mercaptopyruvate sulfur-transferase, can also generate  $H_2S$ . Within a vessel, CGL is the most abundant  $H_2S$ -producing enzyme in ECs,<sup>38</sup> and ECs lacking CGL display increased monocyte adhesion and susceptibility to atherogenesis.<sup>39</sup>  $H_2S$  exerts proangiogenic<sup>40</sup> and cytoprotective effects on ECs<sup>41</sup> and limits leucocyte attachment to the endothelium.<sup>42</sup> It is also a potent vasodilator<sup>43</sup> and inhibitor of vascular smooth muscle cell (VSMC) proliferation,<sup>44</sup> thereby showing therapeutic potential in vein graft disease.

While reducing total calorie intake prior to elective surgery could prove difficult for patients with cardiovascular disease, similar benefits have been achieved in pre-clinical models via restriction of protein or sulfur amino acids in rodent models of renal or hepatic ischaemia–reperfusion injury and femoral ligation.<sup>26,29,31,45</sup> Here, we tested the hypothesis that dietary preconditioning with an isocaloric protein-free diet for one week prior to surgery will attenuate vein graft IH via increased CGL expression and  $H_2S$  production.

## 2. Methods

### 2.1 Experimental animals

All animal experiments were approved by the appropriate Harvard Medical Area or Brigham and Women's Hospital Institutional Animal Care and Use Committee (04475 or A4752-01) and in accordance with NIH guidelines. Surgical vein graft experiments were performed on low-density lipoprotein receptor knockout ( $LDLR^{-/-}$ ) mice (male, 10–12 weeks old, B6.129S7- $LDLr^{tm1Her}$ , Stock No: 002207, Jackson Laboratory,  $n = 10–18$  per group), CGL<sup>tg</sup> mice (male, 10–12 weeks old, hemizygous for bacterial artificial chromosome containing CGL, described in more detail below, on a C57BL/6J background) vs. (littermate non-transgenic controls,  $n = 5–8$  per group), or C57BL/6J (male, 10–12 weeks old, Stock No: 000664, Jackson Laboratory). For dietary preconditioning baseline studies either male  $LDLR^{-/-}$  or C57BL/6J (male, 10–12 weeks old, Stock No: 000664, Jackson Laboratory) mice were used. Mice were housed 4–5 per cage and maintained on a 12-h light-dark cycle at 22°C with 30–50% humidity.

### 2.2 Construction of CGL BAC transgenic model

BAC RP24-344N5 containing the CGL/CTH/CSE locus from the RPCI-24 BAC library on a male C57BL/6J background was obtained from CHORI. The highly active *Ankrd13c* promoter located approximately 20 kb upstream and antisense to the CGL promoter was removed by first inserting a cassette containing a *NotI*-FRT-kan/*neo*-FRT restriction site ~4 kb upstream of the *Ankrd13c* promoter by RedET recombination, and then digesting the resulting BAC with *NotI*. This released a 157 kb fragment containing CGL with 18 kb upstream and over 100 kb downstream of the CGL CDS, but with no other exon sequences present. This fragment was isolated by pulse field gel electrophoresis, purified and injected into C57BL/6J oocytes. A single founder line was identified by PCR using primers 2981 (CTH Common F: TGGGACAGCTCTTCTCCCTTA), 2982 (CTH Tg R: GCAGAATTCACCACTGGACTA) and 2983 (CTH WT R: TTCTGTGAGGAGGGAGCCAT) resulting in a 577 bp control band from the WT allele, and a 369 bp band from the BAC transgene. Based on mRNA and protein analysis, we predict insertion of at least two copies of the BAC into an unknown location in the genome. The BAC transgene array was maintained by breeding non-transgenic to hemizygous BAC-transgenic animals and using hemizygous BAC-tg vs. WT littermate controls in all experiments.

### 2.3 Diets

Upon arrival, mice were acclimated to the animal facility for 3 days, and subsequently fed a complete high-fat high-cholesterol (HFHC) diet (20% Kcal protein, 40% Kcal carbohydrates, 40% Kcal fat, 1.25% cholesterol, Research Diets, New Brunswick, NJ, Diet D12108C) on an *ad libitum*

basis in order to mimic the hyperlipidaemic status of the typical vascular surgery patient with occlusive arterial disease. Following 3 weeks of HFHC feeding, after which blood cholesterol values are stabilized,<sup>46</sup> cages were randomized into the following groups: HFHC donors, HFHC recipients, PR-HFHC donors, and PR-HFHC recipients. PR-HFHC diets consisted of a HFHC base in which all protein was isocalorically replaced with carbohydrates (0% Kcal protein, 60% Kcal carbohydrates, 40% Kcal fat, 1.25% cholesterol, Research Diets, New Brunswick, NJ, Diet D16082403). These diets were continued for 1 week prior to surgery. Vein grafts were performed in PR-HFHC or HFHC recipient mice with thoracic inferior vena cava (IVC) from donor mice treated with the same dietary intervention (either complete HFHC or PR-HFHC). To test the effects of donor vs. recipient, only the donor or recipient mouse was fed PR-HFHC for 7 days. Immediately following surgery all groups resumed the complete HFHC diet. Mice were weighed weekly.

In a separate experiment, LDLR<sup>-/-</sup> mice were injected with either vehicle (0.9% sodium chloride) or the CGL inhibitor DL-propargylglycine (PAG, Sigma Aldrich, 10–20 mg/kg intra-peritoneal daily for 7 days) during a week of dietary intervention (PR + vehicle, PR + PAG) and were either euthanized after 7 days of dietary intervention or were subjected to vein graft surgery and euthanized 28 days after surgery.

## 2.4 Vein graft surgery

Interposition vein graft surgery was performed as previously described.<sup>47</sup> In brief, the mouse was anaesthetized with 3–5% isoflurane and maintained under nose-cone with continuous 1.5–3% isoflurane inhalation. Hair was removed, area sterilized and a midline neckline incision was performed. The right common carotid artery (CCA) was dissected, ligated midway with an 8-0 nylon suture and then divided. The CCA was clamped proximally and distally and a polyetheretherketone cuff was placed on the proximal and distal arterial ends. The arterial lumen was then everted over the cuffs. The thoracic IVC from a donor mouse was harvested, sleeved over the cuffs and secured by 8-0 nylon sutures. Proximal and distal clamps were removed and patency of the graft was confirmed by visual inspection. The incision was closed with 6-0 vicryl sutures. Post-operatively animals received warm lactate ringer solution (0.5–1.0 mL, subcutaneous) and buprenorphine (0.1 mg/kg, subcutaneous).

## 2.5 Duplex ultrasound biomicroscopy

High-resolution ultrasonography was performed *in vivo* on mouse vein grafts at Day 28 using a Vevo 2100 imaging system with 18- to 70-MHz linear array transducers (VisualSonics Inc., Toronto, ON, Canada). Mice were anaesthetized with inhaled isoflurane, and body temperature was maintained using a 37°C heated stage. M-mode was used for vessel cross-sectional dimensions. Three luminal axial images were performed (proximal, distal, and mid vein graft), and mean vessel luminal diameters were calculated.

## 2.6 Vein graft analysis

Experimental endpoints were analysed at baseline, Day 4 or Day 28 after surgery. Whole blood was obtained via percutaneous heart puncture in anaesthetized mice, which were then perfused with lactate Ringers solution for 3 min and perfusion-fixed with 10% formalin for 3 min. For harvest of vein grafts, the neck was opened, and the graft was harvested en-bloc and fixed in 3% formaldehyde in PBS for 24 h or frozen in OCT (Tissue Tek) for immunohistochemistry. IVCs and thoracic aortas were used for isolation of primary ECs or flash frozen for isolation of protein/RNA.

## 2.7 Tissue processing and histology

Vein grafts embedded in OCT compound were cut in 5 µm sections by cryotome. Formalin fixed vein grafts were transferred to 70% ethanol, embedded into paraffin blocks, and then cut using a microtome in 5 µm thick cross sections at regular 200 µm intervals starting from the proximal cuff. Cross sections were mounted on slides and Masson trichrome histology staining was performed. In short, slides were deparaffinized to 95% ethanol, stained in 5% picric acid (in 95% ethanol) for 3 min, washed with tap water, stained in working Harris Hematoxylin Solution (Fisher Scientific, cat# 245-678) 3 min, washed with tap water, stained with 1% Biebrich Scarlet in 1% acetic acid (Fisher Scientific, cat# A38S-500) for 3 min, rinsed in distilled water, 5% Phosphomolybdic/Phosphotungstic acid solution for 1 min, stained with 2.5% light green SF yellowish in 2.5% acetic acid (Fisher Scientific, cat# A38S-500) for 4 min, rinsed in distilled water, then in 1% acetic acid solution (Fisher Scientific, cat# A38S-500) for 2 min. Slides were dehydrated with xylene and mounted with cover glass using permount.

## 2.8 Immunohistochemistry

Slides were pre-incubated in a vacuum oven for 30 min at 65°C. Then deparaffinization was performed via consecutive washes in xylene (3 × 5 min), 100% ethanol (3 × 5 min), 75% ethanol (1 × 5 min), 50% ethanol (1 × 5 min). For antigen retrieval, slides were incubated in citrate buffer (Abcam, ab94674) for 30 min at 96°C. After cool down to room temperature (RT), slides were pre-incubated in a 10% goat serum (Life Technologies, #50062Z), 0.3 M glycine (Ajinomoto, #R015N0080039) solution for 1 h at RT. Slides were then incubated with primary antibodies for either SMC-α (mouse anti-mouse, Abcam, ab7817), Neutrophil-elastase (rabbit anti-mouse, Abcam, ab68672), CGL (rabbit anti-mouse, Abcam, ab151769), CBS (rabbit anti-mouse, Abcam, ab135626) or SMC-α SMC-a (mouse anti-mouse, Abcam, ab7817) and Ki-67 (rabbit anti-mouse, Abcam, ab16667) overnight at 4°C. The following day slides were washed in PBS + Tween (0.05%) solution (3 × 5 min). For fluorescent IHC protocols tissues were then stained with secondary antibodies Alexa Fluor 488 (goat anti-rabbit, AA11034), Alexa Fluor 568 (goat anti-rat, A-11077), Alexa Fluor 568 (goat anti-rabbit, A-11011), or Alexa Fluor 647 (goat anti-mouse, A32728) for 2 h at RT. After wash with PBS + Tween (3 × 5 min), slides were mounted with DAPI (Vector, CB-1000) and imaged. In conventional IHC, after binding primary antibodies with secondary biotinylated goat anti-rat (Vector Laboratories, BA-9401), goat anti-mouse (Vector Laboratories, BA-9200), or goat anti-rabbit (Vector Laboratories, BA-1000) antibodies for 2 h at RT, slides were incubated with ABC-complex (Vectastain, PK-7100) for 30 min at RT. Slides were then washed with PBS (3 × 5 min) and incubated with a DAB peroxidase substrate kit (Vector, SK-4100) for various time-periods depending on the manufacturers protocol. Slides were then dehydrated via consecutive washes in 50% Ethanol (1 × 5 min), 70% Ethanol (1 × 5 min), 100% Ethanol (3 × 5 min), Xylene (3 × 5 min), mounted with Permount (Fischer Scientific) and imaged. For IHC on frozen tissue embedded in OCT slides were defrosted at RT, fixed in 4% paraformaldehyde, washed in phosphate buffered saline (PBS) and then permeabilized (PBS, 0.2% Triton-X). Slides were incubated in 10% goat serum then incubated with primary antibody (neutrophil anti-elastase) overnight at 4°C. The following day slides were washed in PBS + tween (0.05%) solution (3 × 5 min), incubated with the secondary antibody Alexa Fluor 568 (goat anti-rabbit, A-11011) for 2 h at RT. Slides were subsequently washed with PBS, stained with DAPI and imaged.



## 2.9 Histology and immunohistochemistry analysis

Slides were imaged using a Zeiss Axio A1 microscope (Carl Zeiss) and histomorphometric and immunohistochemistry analysis was performed in ImageJ 1.51p (Java 1.8.0\_66). All histological and immunohistochemical analysis were performed by a blinded observer. Histology analysis consisted of five slides per graft, 200  $\mu\text{m}$  apart beginning from the proximal cuff, with three cross-sections per slide. Luminal, intimal, medial, and adventitial areas and circumferences were measured from each cross-section, mean value was calculated per slide and consecutively per vein graft. Intimal area and thickness, medial+adventitial (M+A) area and thickness, intimal vs. medial+adventitial (I/M+A) area and I/M+A thickness ratios were calculated. For collagen content of intimal and M+A layers, Masson trichome stained slides were processed in ImageJ by colour-deconvolution and percentage of green stained area compared with total area was calculated. Immunohistochemical analysis consisted of one slide per venous graft, at a distance of 400  $\mu\text{m}$  from the proximal cuff. For smooth muscle cell (SMC- $\alpha$ ) proliferation, the intimal and (M+A) area occupied by SMC- $\alpha$  stained cells were calculated via the colour deconvolution function in ImageJ. Cells co-localizing both SMC- $\alpha$  and Ki-67 signal were designated as proliferating SMC and manually counted. Neutrophil-elastase positive cells were manually counted employing ImageJ and normalized by area (in  $\text{mm}^2$ ) of each vein graft layer.

## 2.10 qPCR/mRNA analysis

Whole tissue samples were homogenized in five volumes of RNA-BEE (Tel Test B labs, #173107-521) using a tissue homogenizer, after which samples were centrifuged at 12 000 $\times$ g at 4°C for 10 min. Supernatant was then transferred to a 1.5 mL Eppendorf tube, combined with 200  $\mu\text{L}$  chloroform (Sigma-Aldrich, #288306-1L) and vortexed. After 5 min of incubation on ice, samples were centrifuged at 12 000 $\times$ g at 4°C for 15 min. The aqueous layer was collected in a fresh tube on ice and one volume of isopropanol was added per sample, then centrifuged (12 000 $\times$ g at 4°C for 10 min). After aspiration of supernatant, 1 mL 75% ethanol was added to each tube, vortexed and then centrifuged (12 000 $\times$ g at 4°C for 10 min). After aspirating the supernatant, RNA pellets were left to dry until partially translucent. Pellets were resuspended in 20  $\mu\text{L}$  RNAase free  $\text{H}_2\text{O}$  and stored at -80°C. cDNA was synthesized using Verso cDNA kit (Thermo #AB-1453/B) according to manufacturer's instructions. qRT-PCR was then performed using SYBR green master mix (BioRad #1725274) and fold changes were calculated using the delta CT method with each sample normalized to B2m and 18s housekeeping genes. 18s primers used were F(GTAACCCGTTGAACCCATT) and R(CCATCCAATCGGTAGTAGCG), B2m primers used were F(CGGCCTGTATGCTATCCAGA) and R(GGGTGAATTCAGTGTGAGCC), Cgl primers used were F(TTGATCGAAACACCCACA) and R(AGCCGACTATTGAGGTCATCA), and Atf4 primers used were F(TCGATGCTCTGTTTCGAATG) and R(AGAATGTAAAGGGGCAACC).

## 2.11 Intracellular $\text{H}_2\text{S}$ determination in endothelial cells by flow cytometry

Due to low EC yield from murine vessels (e.g. aorta, IVC, carotid artery) lungs were used to obtain a single cell suspension as previously described.<sup>48</sup> In brief, the organ was harvested and gently minced using a scalpel, placed into media (DMEM, Gibco #11965-092) and then into digestion buffer (DMEM Media, Gibco #11965-092) with 2 mg/mL

collagenase II & IV (Gibco #9001-12-1) for 30 min at RT under continuous horizontal shaking (300 rpm), strained through a 100  $\mu\text{m}$  cell strainer, and then centrifuged for 5 min at 1200 rpm and the supernatant discarded. The resulting cellular pellet was washed with antibody binding buffer (ABB) (2 mM EDTA, 1% fetal bovine serum (Gibco) (FBS), 0.5% BSA, in dPBS) and centrifuged for 5 min at 1200 rpm, then decanted and cells were counted using a hemocytometer and split into respective tubes for staining for flow cytometric analysis. Cells were stained for 30 min in the dark at 4°C with CD31 APC (1  $\mu\text{L}/1 \times 10^6$  cells, Miltenyi Biotec, #130-102-571) for EC staining and P3 to measure intracellular  $\text{H}_2\text{S}$  (10  $\mu\text{M}$  final concentration, Millipore Sigma #595504). Cells were then fixed in 2% paraformaldehyde, washed and analysed using a Fortessa Flow Cytometer (BD Biosciences, San Jose, CA, USA). Controls consisted of an unstained control for compensation and gating as well as single-stained CD31 and single-stained P3 samples. CD31+ cells were used as a stopping gate for events collected by the flow cytometer (10 000 CD31+ cells) to ensure robust EC counts.

## 2.12 Western blotting from vessel and isolated vessel endothelial cells

To evaluate whole vessel protein expression following 1 week of protein restriction compared with control diet, thoracic aortas were surgically dissected (perivascular fat removed) and frozen in liquid nitrogen. Whole aortas were homogenized with passive lysis buffer (Promega #E1941), normalized for protein content using a BCA assay, boiled with SDS loading buffer and separated by SDS-PAGE. Proteins were transferred to a PVDF membrane and blotted for CGL (Abcam, ab151769) and CBS (Abcam, ab135626). Aortas from CGL<sup>-/-</sup> mice were used as a specificity control for the CGL antibody. To assess protein levels from vessel ECs, aortas and IVCs were digested for 30 min at 37°C in collagenase/dispase digestion buffer (200 U/mL collagenase type II Gibco #17101015, dispase Promega #V1891, 1:2 in DMEM) under continuous horizontal shaking (300 rpm). After 30 min, an equal volume of complete DMEM with 10% FBS (Thermo Fisher #10082147) was added, and the cell mixture was passed through a 100  $\mu\text{m}$  cell strainer, centrifuged (5 min, 1200 rpm 4°C) and digestion and centrifugation were repeated as above. After supernatant removal, the cell pellet was resuspended in ABB and consecutively incubated with 10  $\mu\text{L}$  FC blocker for 10 min, 10  $\mu\text{L}$  APC conjugated CD31 (Miltenyi Biotec, #130-102-571) for 15 min, 20  $\mu\text{L}$  selection cocktail for 15 min, and then magnetic particles (10  $\mu\text{L}$ ) were added. The tube was incubated in a cell separation magnet (Stemcell technologies, #18000) for 5 min, supernatant removed, and the pellet resuspended in 2.5 mL ABB. After repeating three magnet incubations totalling 15 min, the isolated ECs were resuspended in passive lysis buffer (Promega #E1941) and western blot was performed as described above.

## 2.13 Lead acetate method for $\text{H}_2\text{S}$ production capacity measurement

$\text{H}_2\text{S}$  production capacity was measured using fresh or frozen tissue homogenized in passive lysis buffer as previously described.<sup>49</sup> In brief, tissue homogenate was normalized for protein content and supplemented with 10 mM cysteine and 1 mM pyridoxal phosphate (PLP) in PBS in a 96 or 384 well plate. Lead acetate detection paper was placed on top of the plate and incubated for 2–4 h at 37°C until lead sulfide darkening of the paper occurred.

## 2.14 Plasma lipid measurement

Circulating plasma lipids were measured following 1 week of dietary intervention using the Piccolo Lipid Panel Plus and the Piccolo Xpress chemistry analyzer following the manufacturer's instructions (Abaxis, Germany).

## 2.15 Statistical analyses

Data are expressed as mean  $\pm$  standard error of the mean (mean  $\pm$  SEM). Normality testing was performed using Shapiro–Wilk; normally distributed data was analysed by Student's *t*-test, one-way or two-way ANOVA, and non-normally distributed data by Mann–Whitney or Kruskal–Wallis test using GraphPad Prism (7.0b).

## 3. Results

### 3.1 Short-term protein restriction attenuates vein graft disease

We first examined whether PR attenuates IH (Figure 1A, schematic of IH development) in a validated surgical model of vein graft disease (donor vein graft harvested from separate mouse) using LDLr<sup>-/-</sup> mice fed a HFHC diet for 3 weeks to model the hyperlipidaemic state of patients with arterial occlusive disease. One week prior to surgery, the experimental group (donors and recipients) were preconditioned on an isocaloric HFHC diet lacking protein (PR-HFHC), while the control mice were maintained on the complete 20% protein HFHC diet. Immediately after surgery, both groups resumed feeding on complete HFHC diet (Figure 1B, dietary intervention). During the dietary intervention, PR-HFHC mice lost approximately 20% of their starting body weight despite no significant difference in food intake per gram of bodyweight or per cage (Supplementary material online, Figure S1A–C). Circulating lipid profiles of mice were unchanged as a function of protein restriction in this hyperlipidaemic mouse model (Supplementary material online, Figure S1D–F).

Vein graft wall adaptations assessed via histo-morphometric vessel analysis at 28 days post-operatively showed significant beneficial effects of dietary preconditioning (Figure 1C). Intimal/medial + adventitial (I/M+A) area ratios ( $P < 0.0001$ , Figure 1D) and thickness ratios ( $P < 0.0001$ , Figure 1E) were significantly lower in the PR-HFHC group compared with the control group. Intimal area was significantly reduced ( $P = 0.0294$ , Figure 1F), while intimal thickness trended lower (Figure 1G) in the PR-HFHC group. This was concomitant with an increase in M+A area ( $P < 0.0001$ , Figure 1F) and thickness ( $P < 0.0001$ , Figure 1G) in the PR-HFHC group. Taken together, these data demonstrate that short-term preoperative PR attenuates vein graft disease in a rodent model.

### 3.2 Preoperative protein restriction limits smooth muscle cell migration and inhibits leucocyte transmigration

EC damage and consequent influx of circulating inflammatory cells are hallmarks of early vein graft adaptations, resulting in IH and loss of graft patency via a fibroproliferative response of VSMCs and migration into the intimal layer within 28 days (Figure 2A and B).<sup>50</sup> Preconditioning on PR significantly reduced the percentage of VSMCs in the intima ( $P = 0.0466$ , Figure 2B) despite a trend toward increased number of proliferating cells in this layer (Figure 2C). PR grafts showed no difference in collagen content vs. control grafts in the intimal or M+A layers (Figure 2D).

To investigate early vein graft adaptations giving rise to a differential VSMC fibroproliferative response between diet groups, grafts were harvested on post-operative Day 4. PR-HFHC fed mice lost about 20% of their starting weight during the dietary intervention, but as early as post-operative Day 4 there were no differences in body weight between the dietary groups (Supplementary material online, Figure S1G). No differences were observed in percent area occupied by VSMCs or Ki-67 positive cells in intimal and adventitia + perivascular adipose tissue (PVAT) layers between dietary preconditioning regimens at this early time point after surgery (Figure 2E–G). However, neutrophil anti-elastase staining was significantly reduced upon PR relative to controls in the intimal layer ( $P = 0.0184$ , Figure 2H and I), adventitial + perivascular adipose tissue (PVAT) layer ( $P = 0.0077$ , Figure 2I) as well as in the total vein graft wall ( $P = 0.0146$ , Figure 2I) consistent with an overall decrease in neutrophil transmigration. Thus, reduced IH observed 28 days after vein grafting in the PR group was associated with a reduced inflammatory response during early vein graft adaptations.

### 3.3 Contribution of donor and recipient response to protein restriction in attenuation of vein graft disease

Because thoracic IVC graft donors and recipients are separate mice, we were next able to determine whether the effects of PR were specific to the donor mouse, the recipient or both. Grafts from donors preconditioned on PR and transplanted into recipients on the control diet displayed no statistically significant attenuation of I/M+A area ratio 28 days after surgery (Figure 3A) relative to grafts in which both donor and recipient were fed a control HFHC diet (data from Figure 1). However, grafts from donors fed a control HFHC diet and transplanted into recipients preconditioned on PR displayed significant attenuation of I/M+A area ratio relative to the same control group ( $P = 0.0036$ , Figure 3A). This effect appeared due in part to an increase in M+A area after preconditioning of the recipient, combined with a tendency of reduced intimal area upon preconditioning of both donor and recipient, but not either alone (Figure 3B and C). Collagen deposition (Figure 3D and E) and luminal diameters (Figure 3F) were not significantly different between diet groups. Taken together, these data suggest that while the major effect of PR on attenuation of vein graft disease is on the recipient, preconditioning of both the donor vein graft and the recipient are necessary to gain a maximal protective response.

### 3.4 Protein restriction up-regulates CGL and H<sub>2</sub>S levels in endothelial cells

Dietary preconditioning protects against hepatic ischaemia–reperfusion injury and has previously been associated with increased expression of the transsulfuration enzyme CGL and increased production of the cytoprotective molecule, H<sub>2</sub>S.<sup>26</sup> CGL is also the major H<sub>2</sub>S-producing enzyme in ECs<sup>36</sup> and is increased in ECs in response to reduced dietary sulfur amino acids.<sup>45</sup> To test the potential role of CGL/H<sub>2</sub>S in PR-mediated protection against vein graft disease, we examined localization and expression of CGL as well as CBS, another major H<sub>2</sub>S producing enzyme, in vessels. Immunohistochemical analysis of IVCs revealed CBS localization primarily in the medial layer (Figure 4A) and CGL in the endothelium (Figure 4B). Quantitation of protein expression by western blot in extracts of whole thoracic aortas revealed a significant increase in both CGL ( $P = 0.014$ , Figure 4C and D) and CBS ( $P = 0.021$ , Figure 4C and D) upon PR-HFHC. However, in ECs isolated from thoracic aortas and IVCs using CD31+ magnetic bead separation, only CGL protein

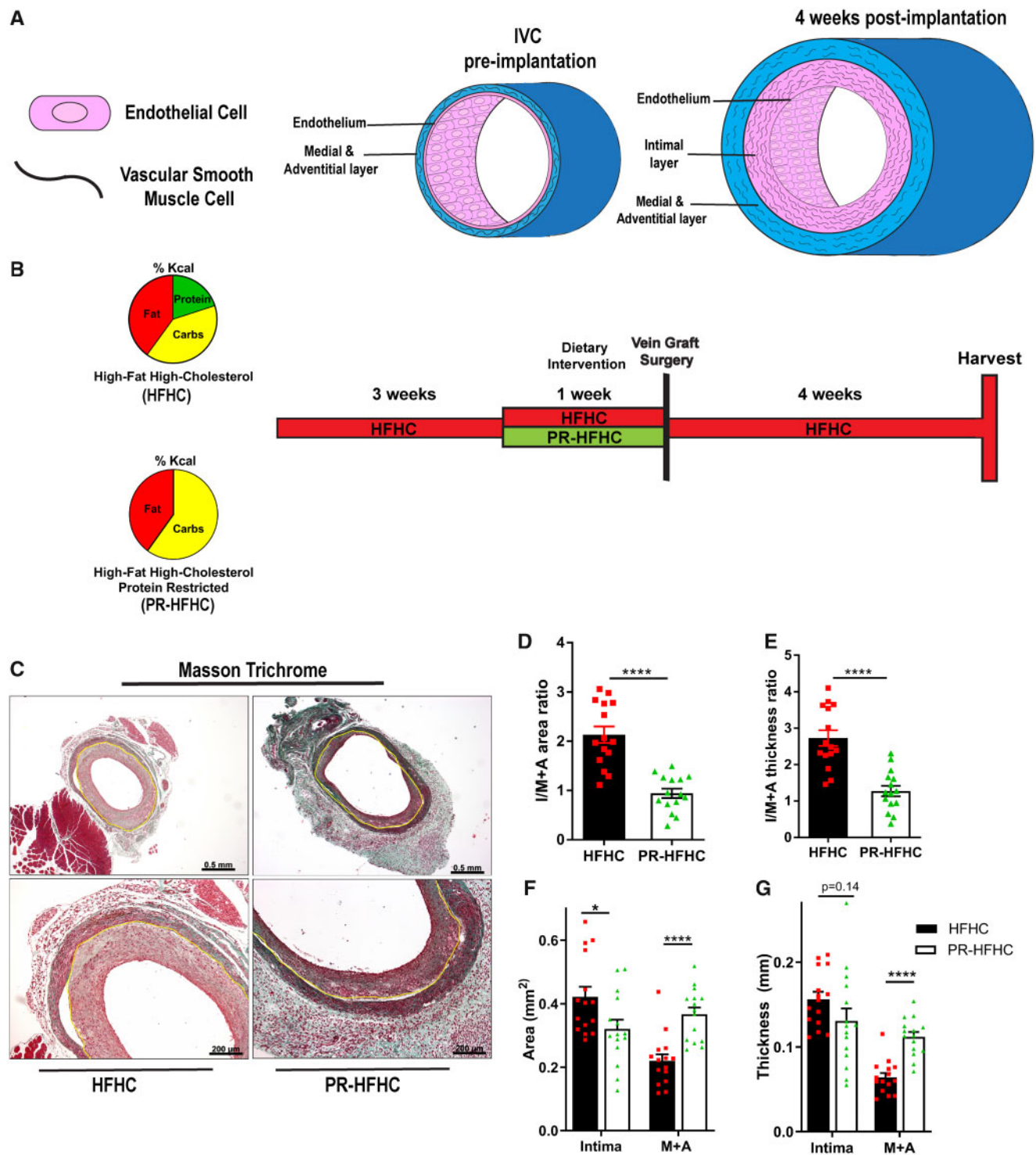


**Figure 1** Short-term protein restriction attenuates vein graft disease. (A) Schematic representation of the development of intimal hyperplasia 4 weeks after implantation of a vein graft (inferior vein cava, IVC) from a separate donor mouse. (B) Schematic representation of diets (left) and dietary alterations (right) during the 3 week run-in, 1 week preconditioning, and 4 week post-operative periods. All mice were subjected to a 3-week run-in period on a HFHC diet. (C) Representative images of Masson trichrome-stained vein grafts 28 days after surgery. Boundary between intimal (I) and medial + adventitial (M+A) layers is traced in yellow. Scale bars = 0.5 mm or 200  $\mu$ m as indicated. (D–G) Vein grafts assessments 28 days after surgery in HFHC vs. PR-HFHC preconditioned mice as indicated;  $n = 15$ /group. (D) I/M+A area ratios ( $2.1 \pm 0.2$  vs.  $0.9 \pm 0.1$ ,  $P < 0.0001$ , Student's  $t$ -test). (E) I/M+A thickness ratios ( $2.7 \pm 0.2$  vs.  $1.2 \pm 0.1$ ,  $P < 0.0001$ , Student's  $t$ -test). (F) Intimal area ( $0.422 \text{ mm}^2 \pm 0.03$  vs.  $0.320 \text{ mm}^2 \pm 0.029$ ,  $P = 0.0294$ , Mann–Whitney test) and M+A area ( $0.22 \text{ mm}^2 \pm 0.021$  vs.  $0.367 \text{ mm}^2 \pm 0.021$ ,  $P < 0.001$ , Student's  $t$ -test). (G) Intimal thickness ( $0.156 \text{ mm} \pm 0.009$  vs.  $0.131 \text{ mm} \pm 0.015$ ) and M+A thickness ( $0.064 \text{ mm} \pm 0.005$  vs.  $0.112 \text{ mm} \pm 0.006$ ,  $P < 0.0001$ , Student's  $t$ -test). All data expressed as mean  $\pm$  SEM; \* $P < 0.05$ , \*\*\*\* $P < 0.0001$ .



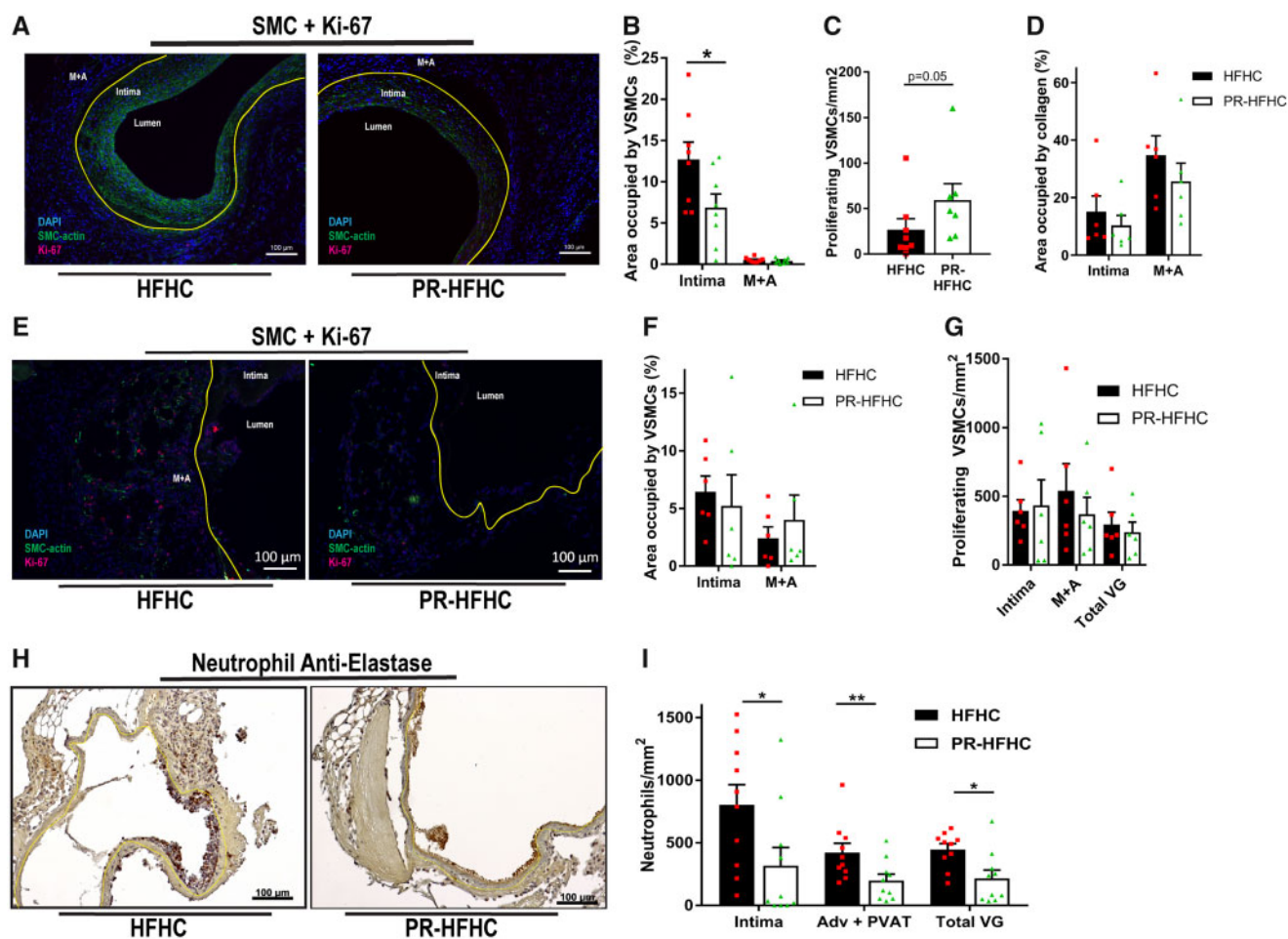


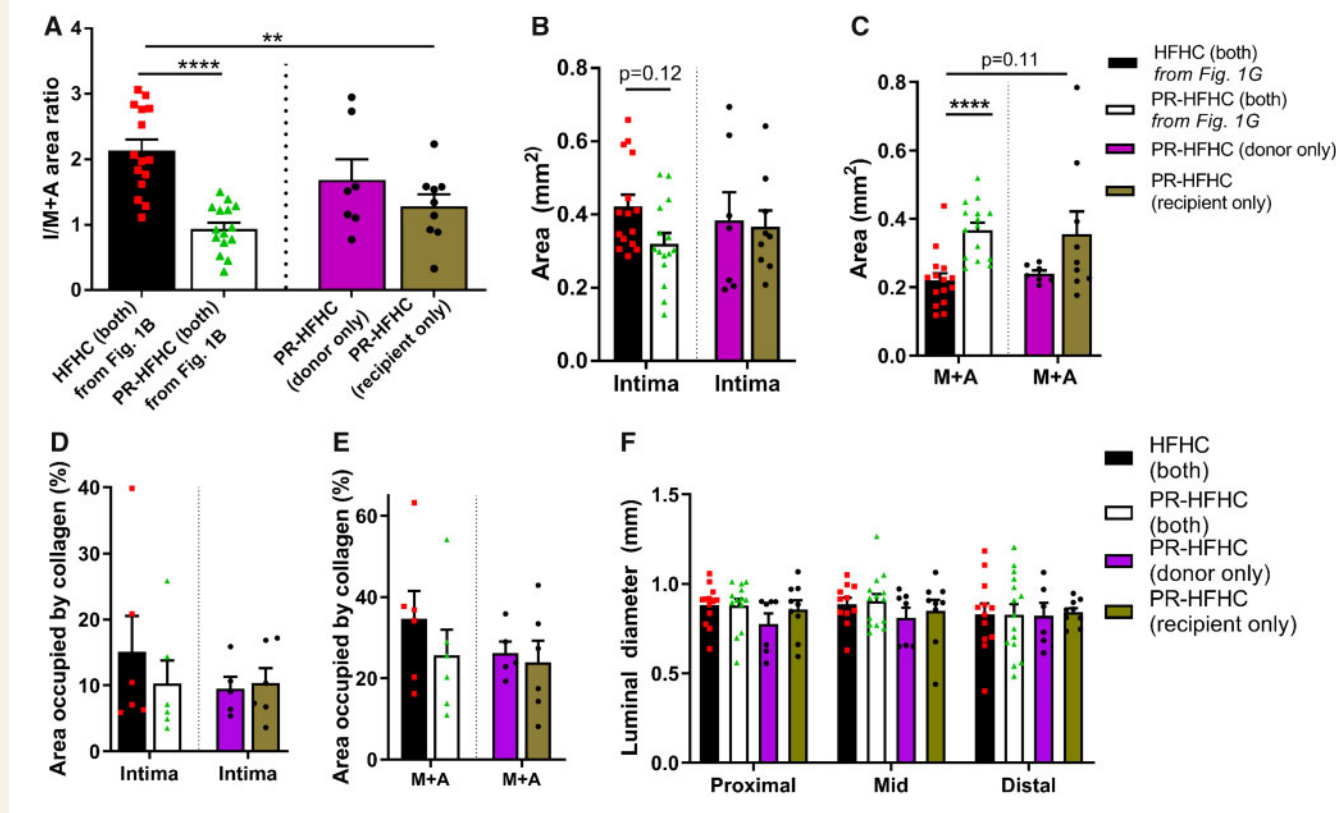
**Figure 2** Preoperative protein restriction limits smooth muscle cell migration and inhibits leucocyte transmigration. (A–I) Assessment of intimal hyperplasia and neutrophil infiltration in vein grafts 28 days (A–D) or 4 days (E–I) after surgery in  $LDLr^{-/-}$  mice preconditioned on the indicated diets;  $n = 5$ –10/group. (A) Representative images of SMC- $\alpha$  (green), Ki-67 (red), and DAPI (blue) stained vein grafts. Included are lumen, intima and media + adventitia as histological landmarks and the intima/M+A border is illustrated by yellow lining. (B) SMC- $\alpha$  positive cells in intimal layer ( $12.7 \pm 2.1$  vs.  $6.9 \pm 1.6$ ;  $P = 0.0446$ , Student's *t*-test) or M+A layer expressed as a percentage of area occupied. (C) Number of proliferating SMC- $\alpha$  and Ki-67 double positive cells in the intimal layer per  $mm^2$  (Student's *t*-test). (D) Percentage of intimal and M+A area occupied by collagen. (E) Representative images of SMC- $\alpha$  (green), Ki-67 (red), and DAPI (blue) stained vein grafts from  $LDLr^{-/-}$  mice preconditioned as indicated and analysed on post-operative Day 4. Included are lumen, intima and M+A as histological landmarks and the Intima/M+A border is illustrated by a yellow line. (F) SMC- $\alpha$  positive cells in intimal or M+A layer expressed as a percentage of area occupied. (G) Number of proliferating SMC- $\alpha$  and Ki-67 double positive cells in the indicated layer per  $mm^2$ . (H) Representative images of neutrophil anti-elastase (brown)-stained vein grafts from  $LDLr^{-/-}$  mice preconditioned as indicated and analysed on post-operative Day 4, with the intima/M+A border depicted by a yellow line. (I) Quantitation of neutrophil transmigration in intimal layer ( $805 \pm 160$  vs.  $322 \pm 131$  cells/ $mm^2$ ,  $P = 0.0184$ , Mann–Whitney test), perivascular adipose tissue (PVAT) layer ( $423 \pm 73$  vs.  $220 \pm 50$  cells/ $mm^2$ ,  $P = 0.0077$ , Student's *t*-test), and total vein graft ( $447 \pm 45$  vs.  $233 \pm 61$  cells/ $mm^2$ ,  $P = 0.0146$ , Student's *t*-test). Scale bars = 100  $\mu m$  as indicated. All data expressed as mean  $\pm$  SEM; \* $P < 0.05$ , \*\* $P < 0.01$ .

expression was significantly increased upon PR (aortic ECs,  $P = 0.02$ , Figure 4E and F; IVC ECs,  $P = 0.01$ , Figure 4G and H). Aortic CGL expression was also significantly increased on the mRNA level in the PR group ( $P = 0.015$ , Figure 4I), as was the transcription factor ATF4 that regulates CGL expression ( $P = 0.044$ , Figure 4J).

We next measured endogenous  $H_2S$  levels in ECs by flow cytometry using a fluorescent  $H_2S$ -specific probe.<sup>51</sup> Due to the limited number of ECs in large vessels, ECs were isolated from lungs of  $LDLr^{-/-}$  mice after 1 week of control HFHC or PR-HFHC diet feeding. A separate group of PR mice was treated with the CGL inhibitor PAG (daily 20 mg/kg IP

injection) to inform on CGL-dependent  $H_2S$  production. While there was no difference in mean fluorescent P3 intensity (Figure 4K and L) amongst groups, there was an increase in the number of CD31+/P3+ cells in the PR-HFHC group ( $P = 0.031$ , Figure 4K, M) that was prevented by PAG treatment ( $P = 0.04$ , Figure 4K, M). Interestingly, CGL and ATF4 gene expression remained significantly increased relative to controls in the PAG treatment group, consistent with the post-translational mechanism of PAG action (Figure 4I and J). Taken together, these data suggest that PR significantly increases CGL protein expression and sulfide production specifically in vascular ECs.





### 3.5 CGL is required for protein restriction mediated attenuation of intimal hyperplasia

To assess the requirement of CGL activity in the attenuation of IH by PR *in vivo*, donor and recipient  $LDLR^{-/-}$  mice injected with either vehicle or PAG during 1 week of dietary preconditioning (PR + PAG vs. PR + vehicle, 10 mg/kg IP) underwent vein graft surgery and post-operative Day 28 harvest and assessment. PAG-treated mice showed increased I/M+A area ( $P = 0.014$ , Figure 5A and B) and thickness ratios ( $P = 0.0144$ , Figure 5C) with trends toward increased intimal thickness and decreased M+A area and thickness (Figure 5D and E) compared to vehicle-treated controls. These data suggest that CGL is required for the attenuation of IH by PR during the preconditioning period.

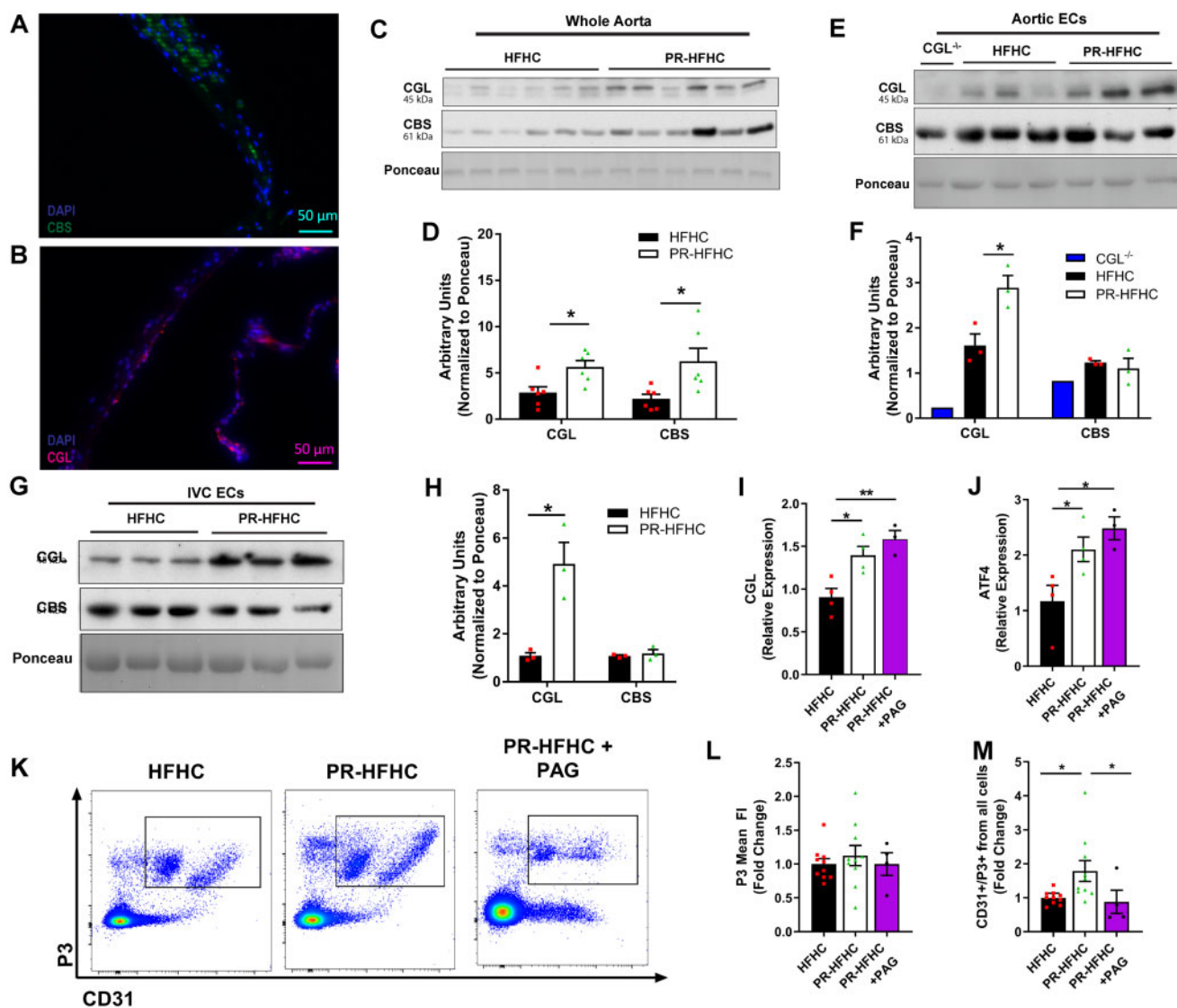
### 3.6 CGL overexpression protects against vein graft disease but does not increase basal endothelial cell $H_2S$ levels

Finally, we asked whether overexpression of CGL could mimic the effects of dietary protein restriction on vein graft disease. For this we engineered a new bacterial artificial chromosome-based CGL transgenic

model (CGL<sup>tg</sup>) containing extra copies of the CGL gene but with endogenous regulatory elements up to 20 kb upstream and over 100 kb downstream intact. Increased CGL protein expression (Figure 6A and B) and  $H_2S$  production capacity (Figure 6C and D) were confirmed in protein extracts of kidney and liver, respectively, relative to non-transgenic littermate controls. CGL protein was also increased in aortic ECs from CGL<sup>tg</sup> mice relative to control mice (data not shown).

To test the effects of CGL overexpression on vein graft disease, CGL<sup>tg</sup> and wild type littermate control mice were placed on a HFHC diet for 3 weeks and then subjected to vein graft surgery. Grafts harvested 28 days after surgery revealed decreased I/M+A area ratio ( $P = 0.0066$ , Figure 6E and F) and thickness ratio ( $P = 0.0159$ , Figure 6G) and reduced intimal SMC- $\alpha$  in CGL<sup>tg</sup> mice ( $P = 0.032$ , Figure 6J and K). Duplex biomicroscopy performed during the 4th post-operative week revealed a trend toward increased distal luminal diameter in CGL<sup>tg</sup> compared with WT mice (Figure 6L) consistent with an outward remodelling phenotype. Furthermore, at post-operative day 4 there was a trend toward reduced intimal neutrophil transmigration in the CGL<sup>tg</sup> compared to WT mice (Figure 6M and N).

Finally, an assessment of endogenous  $H_2S$  levels in ECs did not reveal any significant differences in mean fluorescent P3 intensity or the number

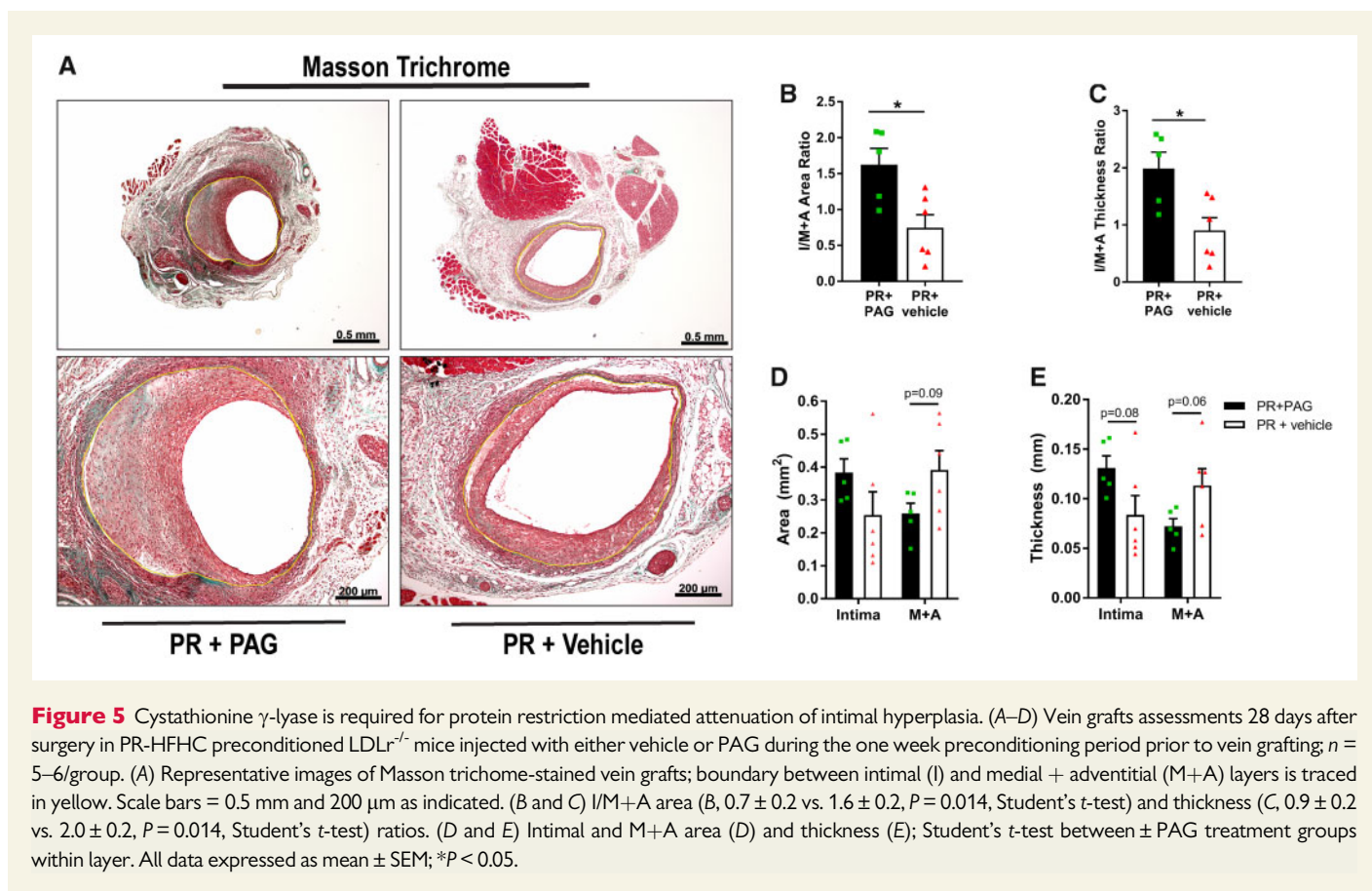


of CD31+/P3+ cells between genotypes (Figure 6O–Q). Taken together, these data suggest that PR and genetic CGL overexpression both attenuate vein graft disease through partially overlapping mechanisms.

## 4. Discussion

Here, we tested a dietary intervention involving unlimited access to food in which protein was entirely replaced with carbohydrates for 1 week, a

paradigm that may be more practical for patients than one involving overall food restriction. We found that one week of PR prior to surgery significantly attenuated IH in a validated mouse vein graft model. Pharmacological inhibition of CGL-dependent  $H_2S$  production using PAG abrogated PR-mediated protection from IH, while genetic overexpression using a new BAC-based CGL transgenic overexpressing model revealed protection independent of diet. Reduced neutrophil infiltration in the vein graft on post-operative Day 4 consistent with a reduced proinflammatory response, and reduced smooth muscle cell infiltration



into the intima on Day 28 signifying an altered fibroproliferative response,<sup>11</sup> were common to both diet and genetic models of improved vein graft patency. Neutrophil infiltration on Day 4 may occur as a result of local changes in the vessel endothelium, thus linking donor and recipient effects that were both required for maximal protection. A model for the role of CGL in PR-mediated protection against IH is presented in Figure 7.

In support of a potential role of CGL-derived  $H_2S$  in vascular injury, it was recently reported that levels of CGL and  $H_2S$  from lower extremity muscles were decreased in PAD patients compared to controls.<sup>52</sup> Recent evidence also demonstrates increased DNA methylation of the CGL gene in CAD patients undergoing CABG.<sup>53</sup> In mice, CGL ablation worsens IH,<sup>54</sup> possibly due to increased EC activation.<sup>39</sup> Here, we observed a significant increase in CGL (but not CBS) protein expression upon PR specifically in ECs derived from IVC and aorta, while in whole aorta CBS was also increased and consistent with CBS and CGL localization to the medial and endothelial layers, respectively. Unfortunately, low EC yields from vessels prevented a robust analysis of  $H_2S$  levels in these cells by flow cytometry. This was possible in lung-derived EC populations, in which we found an increase in the frequency of P3+ ( $H_2S$ -producing) ECs after one week of PR. However, surprisingly, we did not observe a significant increase in basal  $H_2S$  production (P3 mean fluorescence intensity) in EC or non-EC populations either upon PR or CGL overexpression. These data suggest that changes in  $H_2S$  production induced upon surgical stress either in ECs or other non-EC cell population such as neutrophils may be more important to vascular protection than basal levels per se. Future studies in different cell types over a time course after

vessel implantation are thus required to investigate whether  $H_2S$  production is increased in interventions in which CGL is up-regulated. Non-mutually exclusive possibilities include the importance of stored rather than free pools of  $H_2S$ , which are currently poorly understood, or the role of CGL in *de novo* cysteine production independent of  $H_2S$  generation. Another caveat in the interpretation of these results is the potential functional heterogeneity between vascular beds from a different origin,<sup>55</sup> thereby limiting our assessment of sulfide production in vascular conduit beds after PR based on lung ECs.

While these preclinical data support potential benefits of  $H_2S$  manipulation on the vascular response to injury, several limitations are acknowledged. The time course of IH in the mouse vein graft model is short, and the durability of the protection remains unknown. Furthermore, the ability of PR to protect against IH across a range of co-morbidities often encountered in vascular surgery patient (old age, high incidence of diabetes, etc.) were not tested in our murine model. Finally, specific temporal therapeutic windows for up-regulation of endogenous  $H_2S$  during the peri-operative period for elective procedures remains obscure. Nonetheless, since this strategy may be relevant for other forms of planned vascular injury (endovascular interventions) as well as for organ transplantation, this early work should incite future research to address these limitations.

## 5. Conclusion

In conclusion, here we provide foundational rodent data that a simple, translatable dietary intervention attenuates the vascular proliferative



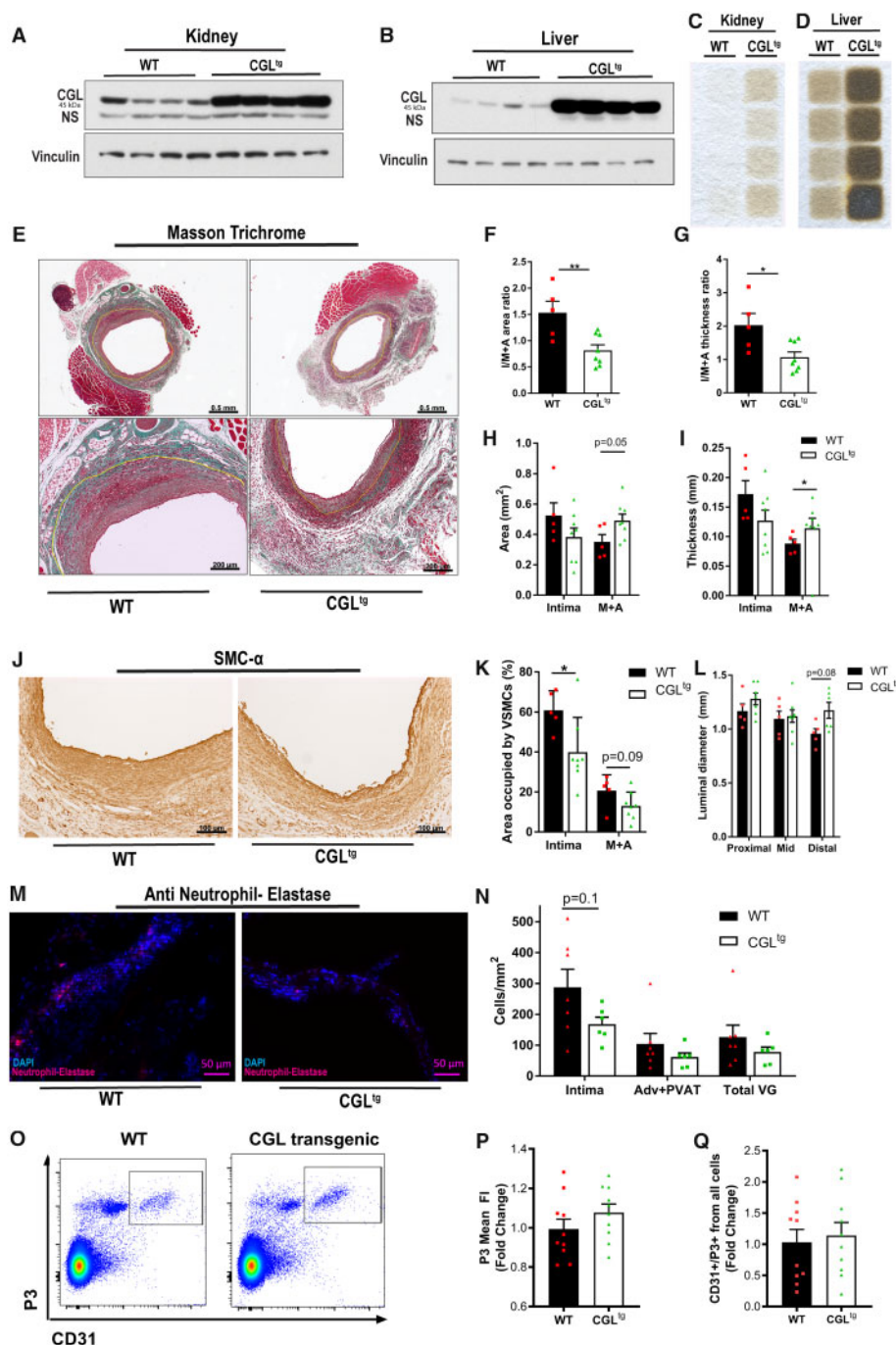
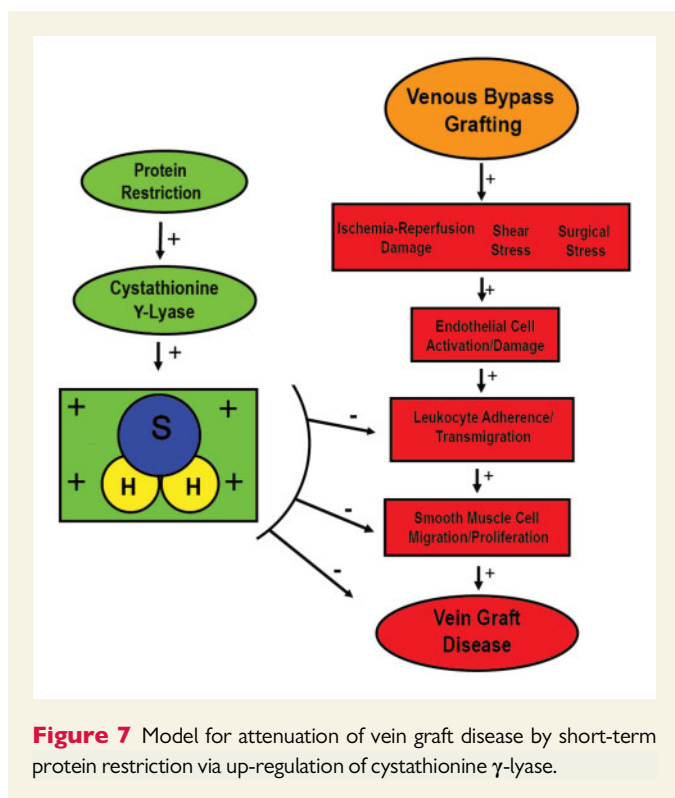


**Figure 6** CGL overexpression protects against vein graft disease but does not increase basal endothelial cell H<sub>2</sub>S levels. (A–D) Western blot of CGL (A and B) and hydrogen sulfide production capacity (C and D) in homogenates of kidney (A, C) and liver (B, D) from hemizygous CGL transgenic (CGL<sup>tg</sup>) and WT littermate mice as indicated. (E–N) Vein grafts assessments in WT vs. CGL<sup>tg</sup> mice ( $n = 5-8$ /group) 28 days (E–L) or 4 days (M–N) after surgery. (E) Representative images of Masson's trichrome-stained vein grafts; boundary between intimal (I) and medial + adventitial (M+A) layers is traced in yellow. Scale bars = 0.5 mm and 200 μm as indicated. (F) I/M+A area ratios ( $1.5 \pm 0.2$  vs.  $0.8 \pm 0.1$ ,  $P = 0.0066$ , Student's *t*-test). (G) I/M+A thickness ratios ( $2.0 \pm 0.4$  vs.  $1.1 \pm 0.2$ ,  $P = 0.0159$ , Student's *t*-test). (H and I) Intimal and M+A area (H) and intimal and M+A thickness (I) ( $0.088 \pm 0.007$  vs.  $0.114 \pm 0.017$ ,  $P = 0.0295$ , Mann-Whitney test). (J) Representative images of vein grafts stained with SMC-α (brown); scale bar = 100 μm. (K) SMC-α positive cells in intimal layer (61 vs. 38,  $P = 0.032$ , Student's *t*-test) or M+A layer expressed as a percentage of area occupied. (L) Vein graft lumen diameter proximal, mid or distal to the heart as indicated (two-way ANOVA with Turkey's multiple comparisons test). (M) Representative images of grafts stained with anti-neutrophil-elastase on post-operative Day 4; scale bars = 50 μm. (N) Quantitation of neutrophil transmigration in intimal layer (Student's *t*-test), adventitial + perivascular adipose tissue (PVAT) layer and total vein graft (Mann-Whitney test). (O–Q) Endogenous H<sub>2</sub>S in lung endothelial cells of WT or CGL<sup>tg</sup> littermates ( $n = 5$ /group). (O) Representative dot plots with CD31/P3 double positive cells indicated within the box. (P, Q) Fold change, relative to WT group, in mean fluorescent intensity of P3 (P) and frequency (Q) of CD31/P3 double positive cells; WT and CGL<sup>tg</sup>  $n = 8-10$ /group; Mann-Whitney test. All data expressed as mean  $\pm$  SEM; \* $P < 0.05$ , \*\* $P < 0.01$ .





response to injury in a clinically relevant model of vein bypass grafting via up-regulation of enzymes directly involved in the production of the cytoprotective gaseous transmitter,  $H_2S$ .

## Supplementary material

Supplementary material is available at *Cardiovascular Research* online.

## Authors contributions

K.M.T. and P.K. conceived of experimental designs, performed experiments and wrote the manuscript. M.T. performed surgeries, collected data, processed and analysed histology. M.R.M. was involved in *ex vivo* experiments, western blot, and data analysis. J.H.T.V. analysed and compensated flow cytometry data. A.L. was involved in transgenic mouse breeding, husbandry, and experimental designs. W.T. and B.N.L. developed the CGL transgenic mouse model. M.R.V. performed CGL transgenic mouse surgeries and advised with P.H.Q. on data analysis of intimal hyperplasia. J.R.M. and C.K.O. provided funding, experimental designs and mentorship and they oversaw the biologic research protocol and organized the necessary collaborations for project completion. They also worked with the co-authors on manuscript preparation and finalization.

**Conflict of interest:** none declared.

## Funding

This work was supported by the Harvard-Longwood Research Training in Vascular Surgery NIH T32 Grant 5T32 HL007734-22 to K.T.; American Heart Association Post-Doctoral Grant [#19POST34400059] and grants from Foundation 'De Drie Lichten', Prins Bernhard Cultural Foundation and

Michael-van Vloten Foundation to P.K.; the Mendez National Institute of Transplantation and the Leenards Foundation to A.L.; American Heart Association Grant-in-Aid 16GRNT27090006; National Institutes of Health, 1R01HL133500 to C.K.O.; and NIH (AG036712, DK090629) and Charoen Pokphand Group to J.R.M.

## References

- Fontana L, Klein S. Aging, adiposity, and calorie restriction. *JAMA* 2007;**297**:986–994.
- Welsh JA, Sharma A, Cunningham SA, Vos MB. Consumption of added sugars and indicators of cardiovascular disease risk among US adolescents. *Circulation* 2011;**123**: 249–257.
- Mente A, de Koning L, Shannon HS, Anand SS. A systematic review of the evidence supporting a causal link between dietary factors and coronary heart disease. *Arch Intern Med* 2009;**169**:659–669.
- Sotos-Prieto M, Bhupathiraju SN, Mattei J, Fung TT, Li Y, Pan A, Willett WC, Rimm EB, Hu FB. Changes in diet quality scores and risk of cardiovascular disease among US men and women. *Circulation* 2015;**132**:2212–2219.
- Weaver H, Shukla N, Ellinsworth D, Jeremy JY. Oxidative stress and vein graft failure: a focus on NADH oxidase, nitric oxide and eicosanoids. *Curr Opin Pharmacol* 2012; **12**:160–165.
- Owens CD, Wake N, Jacot JG, Gerhard-Herman M, Gaccione P, Belkin M, Creager MA, Conte MS. Early biomechanical changes in lower extremity vein grafts—distinct temporal phases of remodeling and wall stiffness. *J Vasc Surg* 2006;**44**:740–746.
- Osgood MJ, Hocking KM, Voskresensky IV, Li FD, Komalavilas P, Cheung-Flynn J, Brophy CM. Surgical vein graft preparation promotes cellular dysfunction, oxidative stress, and intimal hyperplasia in human saphenous vein. *J Vasc Surg* 2014;**60**:202–211.
- Walpole PL, Gotlieb AI, Cybulsky MI, Langille BL. Expression of ICAM-1 and VCAM-1 and monocyte adherence in arteries exposed to altered shear stress. *Arterioscler Thromb Vasc Biol* 1995;**15**:2–10. Published erratum appears in *Arterioscler Thromb Vasc Biol* 1995;**15**:1429.
- Khaleel MS, Dorheim TA, Duryee MJ, Durbin HE, Bussey WD, Garvin RP, Klassen LW, Thiele GM, Anderson DR. High-pressure distention of the saphenous vein during preparation results in increased markers of inflammation: a potential mechanism for graft failure. *Ann Thorac Surg* 2012;**93**:552–558.
- Voisin MB, Nourshargh S. Neutrophil transmigration: emergence of an adhesive cascade within venular walls. *J Innate Immun* 2013;**5**:336–347.
- de Vries MR, Simons KH, Jukema JW, Braun J, Quax P. Vein graft failure: from pathophysiology to clinical outcomes. *Nat Rev Cardiol* 2016;**13**:451–470.
- Ambler GK, Twine CP. Graft type for femoro-popliteal bypass surgery. *Cochrane Database Syst Rev* 2018;**2**:CD001487.
- Conte MS, Bandyk DF, Clowes AW, Moneta GL, Seely L, Lorenz TJ, Namini H, Hamdan AD, Roddy SP, Belkin M, Berclai SA, DeMasi RJ, Samson RH, Berman SS. Results of PREVENT III: a multicenter, randomized trial of edifoligide for the prevention of vein graft failure in lower extremity bypass surgery. *J Vasc Surg* 2006;**43**: 742–751.e741.
- Song HG, Rumma RT, Ozaki CK, Edelman ER, Chen CS. Vascular tissue engineering: progress, challenges, and clinical promise. *Cell Stem Cell* 2018;**22**:340–354.
- Almasri J, Adusumalli J, Asi N, Lakis S, Alsawas M, Prokop LJ, Bradbury A, Kolh P, Conte MS, Murad MH. A systematic review and meta-analysis of revascularization outcomes of infrainguinal chronic limb-threatening ischemia. *J Vasc Surg* 2018;**68**: 624–633.
- Bhatt DL. CABG the clear choice for patients with diabetes and multivessel disease. *Lancet* 2018;**391**:913–914.
- Royce A, Pawanis Z, Canty D, Ou-Young J, Eccleston D, Ajani A, Reid CM, Bellomo R, Royce C. The effect on survival from the use of a saphenous vein graft during coronary bypass surgery: a large cohort study. *Eur J Cardiothorac Surg* 2018;**54**: 1093–1100.
- Burmand KM, Lahiri RP, Burr N, Jansen van Rensburg L, Lewis MP. A randomised, single blinded trial, assessing the effect of a two week preoperative very low calorie diet on laparoscopic cholecystectomy in obese patients. *HPB (Oxford)* 2016;**18**: 456–461.
- van Ginhoven TM, de Bruin RW, Timmermans M, Mitchell JR, Hoeijmakers JH, Ijzerman JN. Pre-operative dietary restriction is feasible in live-kidney donors. *Clin Transplant* 2011;**25**:486–494.
- Fleisher LA, Beckman JA, Brown KA, Calkins H, Chaikof E, Fleischmann KE, Freeman WK, Froehlich JB, Kasper EK, Kersten JR, Riegel B, Robb JF, Smith SC Jr, Jacobs AK, Adams CD, Anderson JL, Antman EM, Buller CE, Creager MA, Ettinger SM, Faxon DP, Fuster V, Halperin JL, Hiratzka LF, Hunt SA, Lytle BW, Nishimura R, Ornato JP, Page RL, Riegel B, Tarkington LG, Yancy CW, ACC/AHA Task Force Members. ACC/AHA 2007 Guidelines on Perioperative Cardiovascular Evaluation and Care for Noncardiac Surgery: executive summary: a report of the American College of Cardiology/American Heart Association Task Force on Practice Guidelines (Writing Committee to Revise the 2002 Guidelines on Perioperative Cardiovascular Evaluation for Noncardiac Surgery): Developed in Collaboration With the American Society of Echocardiography, American Society of Nuclear Cardiology, Heart Rhythm Society, Society of Cardiovascular Anesthesiologists, Society for

- Cardiovascular Angiography and Interventions, Society for Vascular Medicine and Biology, and Society for Vascular Surgery. *Circulation* 2007;**116**:1971–1996.
21. Gallinetti J, Harputlugil E, Mitchell JR. Amino acid sensing in dietary-restriction-mediated longevity: roles of signal-transducing kinases GCN2 and TOR. *Biochem J* 2013;**449**:1–10.
  22. Walford RL, Harris SB, Gunion MW. The calorically restricted low-fat nutrient-dense diet in Biosphere 2 significantly lowers blood glucose, total leukocyte count, cholesterol, and blood pressure in humans. *Proc Natl Acad Sci USA* 1992;**89**:11533–11537.
  23. Longchamp A, Harputlugil E, Corpataux JM, Ozaki CK, Mitchell JR. Is overnight fasting before surgery too much or not enough? How basic aging research can guide preoperative nutritional recommendations to improve surgical outcomes: a mini-review. *Gerontology* 2017;**63**:228–237.
  24. Ej M. Subfield history: caloric restriction, slowing aging, and extending life. *Sci Aging Knowledge Environ* 2003;**2003**:RE2.
  25. Mirzaei H, Di Biase S, Longo VD. Dietary interventions, cardiovascular aging, and disease: animal models and human studies. *Circ Res* 2016;**118**:1612–1625.
  26. Hine C, Harputlugil E, Zhang Y, Ruckstuhl C, Lee BC, Brace L, Longchamp A, Trevino-Villarreal JH, Mejia P, Ozaki CK, Wang R, Gladyshev VN, Madeo F, Mair WB, Mitchell JR. Endogenous hydrogen sulfide production is essential for dietary restriction benefits. *Cell* 2015;**160**:132–144.
  27. Mauro CR, Tao M, Yu P, Trevino-Villarreal JH, Longchamp A, Kristal BS, Ozaki CK, Mitchell JR. Preoperative dietary restriction reduces intimal hyperplasia and protects from ischemia-reperfusion injury. *J Vasc Surg* 2016;**63**:500–509.e1.
  28. Harputlugil E, Hine C, Vargas D, Robertson L, Manning BD, Mitchell JR. The TSC complex is required for the benefits of dietary protein restriction on stress resistance in vivo. *Cell Rep* 2014;**8**:1160–1170.
  29. Peng W, Robertson L, Gallinetti J, Mejia P, Vose S, Charlip A, Chu T, Mitchell JR. Surgical stress resistance induced by single amino acid deprivation requires Gcn2 in mice. *Sci Transl Med* 2012;**4**:118ra11.
  30. Varendi K, Airavaara M, Anttila J, Vose S, Planken A, Saarna M, Mitchell JR, Andressoo JO. Short-term preoperative dietary restriction is neuroprotective in a rat focal stroke model. *PLoS One* 2014;**9**:e93911.
  31. Robertson LT, Treviño-Villarreal JH, Mejia P, Grondin Y, Harputlugil E, Hine C, Vargas D, Zheng H, Ozaki CK, Kristal BS, Simpson SJ, Mitchell JR. Protein and calorie restriction contribute additively to protection from renal ischemia reperfusion injury partly via leptin reduction in male mice. *J Nutr* 2015;**145**:1717–1727.
  32. Trocha K, Kip P, MacArthur MR, Mitchell SJ, Longchamp A, Treviño-Villarreal JH, Tao M, Bredella MA, De Amorim Bernstein K, Mitchell JR, Ozaki CK. Preoperative protein or methionine restriction preserves wound healing and reduces hyperglycemia. *J Surg Res* 2019;**235**:216–222.
  33. Mitchell JR, Verweij M, Brand K, van de Ven M, Goemaere N, van den Engel S, Chu T, Forrer F, Müller C, de Jong M, van Ijcken W, Ijzermans JNM, Hoeijmakers JHJ, de Bruin RWF. Short-term dietary restriction and fasting precondition against ischemia reperfusion injury in mice. *Aging Cell* 2010;**9**:40–53.
  34. Mitchell JR, Beckman JA, Nguyen LL, Ozaki CK. Reducing elective vascular surgery perioperative risk with brief preoperative dietary restriction. *Surgery* 2013;**153**:594–598.
  35. Mejia P, Treviño-Villarreal JH, Hine C, Harputlugil E, Lang S, Calay E, Rogers R, Wirth D, Duraisingh MT, Mitchell JR. Dietary restriction protects against experimental cerebral malaria via leptin modulation and T-cell mTORC1 suppression. *Nat Commun* 2015;**6**:6050.
  36. Yang G, Wu L, Jiang B, Yang W, Qi J, Cao K, Meng Q, Mustafa AK, Mu W, Zhang S, Snyder SH, Wang R. H<sub>2</sub>S as a physiologic vasorelaxant: hypertension in mice with deletion of cystathionine  $\gamma$ -lyase. *Science* 2008;**322**:587–590.
  37. Wallace JL, Blackler RW, Chan MV, Da Silva GJ, Elsheikh W, Flannigan KL, Gamanek I, Manko A, Wang L, Motta JP, Buret AG. Anti-inflammatory and cytoprotective actions of hydrogen sulfide: translation to therapeutics. *Antioxid Redox Signal* 2015;**22**:398–410.
  38. Wang R. Physiological implications of hydrogen sulfide: a Whiff exploration that blossomed. *Physiol Rev* 2012;**92**:791–896.
  39. Bibli SI, Hu J, Sigala F, Wittig I, Heidler J, Zukunf S, Tsilimigras DI, Randriamboavonjy V, Wittig J, Kojonazarov B, Schurmann C, Siragusa M, Siuda D, Luck B, Abdel Malik R, Filiis KA, Zografos G, Chen C, Wang DW, Pfeilschifter J, Brandes RP, Szabo C, Papapetropoulos A, Fleming I. Cystathionine gamma lyase sulphydrates the RNA binding protein Human Antigen R to preserve endothelial cell function and delay atherogenesis. *Circulation* 2018;**139**:101–114.
  40. Papapetropoulos A, Pyriochou A, Altaany Z, Yang G, Marazioti A, Zhou Z, Jeschke MG, Branski LK, Herndon DN, Wang R, Szabo C. Hydrogen sulfide is an endogenous stimulator of angiogenesis. *Proc Natl Acad Sci USA* 2009;**106**:21972–21977.
  41. King AL, Polhemus DJ, Bhushan S, Otsuka H, Kondo K, Nicholson CK, Bradley JM, Islam KN, Calvert JW, Tao YX, Dugas TR, Kelley EE, Elrod JW, Huang PL, Wang R, Lefer DJ. Hydrogen sulfide cytoprotective signaling is endothelial nitric oxide synthase-nitric oxide dependent. *Proc Natl Acad Sci USA* 2014;**111**:3182–3187.
  42. Zano RCO, Brancalione V, Distrutti E, Fiorucci S, Cirino G, Wallace JL. Hydrogen sulfide is an endogenous modulator of leukocyte-mediated inflammation. *FASEB J* 2006;**20**:2118–2120.
  43. Greaney JL, Kutz JL, Shank SW, Jandu S, Santhanam L, Alexander LM. Impaired hydrogen sulfide-mediated vasodilation contributes to microvascular endothelial dysfunction in hypertensive adults. *Hypertension* 2017;**69**:902–909.
  44. Shuang T, Fu M, Yang G, Wu L, Wang R. The interaction of IGF-1/IGF-1R and hydrogen sulfide on the proliferation of mouse primary vascular smooth muscle cells. *Biochem Pharmacol* 2018;**149**:143–152.
  45. Longchamp A, Mirabella T, Arduini A, MacArthur MR, Das A, Treviño-Villarreal JH, Hine C, Ben-Sahra I, Knudsen NH, Brace LE, Reynolds J, Mejia P, Tao M, Sharma G, Wang R, Corpataux JM, Haefliger JA, Ahn KH, Lee CH, Manning BD, Sinclair DA, Chen CS, Ozaki CK, Mitchell JR. Amino acid restriction triggers angiogenesis via GCN2/ATF4 regulation of VEGF and H<sub>2</sub>S production. *Cell* 2018;**173**:117–129.e14.
  46. Kowala MC, Recce R, Beyer S, Gu C, Valentine M. Characterization of atherosclerosis in LDL receptor knockout mice: macrophage accumulation correlates with rapid and sustained expression of aortic MCP-1/JE. *Atherosclerosis* 2000;**149**:323–330.
  47. Yu P, Nguyen BT, Tao M, Campagna C, Ozaki CK. Rationale and practical techniques for mouse models of early vein graft adaptations. *J Vasc Surg* 2010;**52**:444–452.
  48. Jungblut M, Oeltze K, Zehnter I, Hasselmann D, Bosio A. Standardized preparation of single-cell suspensions from mouse lung tissue using the gentleMACS Dissociator. *J Vis Exp* 2009;doi:10.3791/1266.
  49. Hine C, Mitchell JR. Endpoint or kinetic measurement of hydrogen sulfide production capacity in tissue extracts. *Bio Protoc* 2017;**7**: pii:e2382.
  50. de Vries MR, Quax P. Inflammation in vein graft disease. *Front Cardiovasc Med* 2018;**5**: 3.
  51. Singha S, Kim D, Moon H, Wang T, Kim KH, Shin YH, Jung J, Seo E, Lee SJ, Ahn KH. Toward a selective, sensitive, fast-responsive, and biocompatible two-photon probe for hydrogen sulfide in live cells. *Anal Chem* 2015;**87**:1188–1195.
  52. Islam KN, Polhemus DJ, Donnarumma E, Brewster LP, Lefer DJ. Hydrogen sulfide levels and nuclear factor-erythroid 2-related factor 2 (NRF2) activity are attenuated in the setting of critical limb ischemia (CLI). *J Am Heart Assoc* 2015;**4**: pii:e001986.
  53. Giannakopoulou E, Konstantinou F, Ragia G, Tavidou A, Karaglani M, Chatzaki E, Papapetropoulos A, Mikroulis D, Manolopoulos VG. Epigenetics-by-sex interaction for coronary artery disease risk conferred by the cystathionine  $\gamma$ -lyase gene promoter methylation. *OMICS* 2017;**21**:741–748.
  54. Yang G, Li H, Tang G, Wu L, Zhao K, Cao Q, Xu C, Wang R. Increased neointimal formation in cystathionine  $\gamma$ -lyase deficient mice: role of hydrogen sulfide in  $\alpha$ 5 $\beta$ 1-integrin and matrix metalloproteinase-2 expression in smooth muscle cells. *J Mol Cell Cardiol* 2012;**52**:677–688.
  55. Potente M, Makinen T. Vascular heterogeneity and specialization in development and disease. *Nat Rev Mol Cell Biol* 2017;**18**:477–494.